Physicochemical, Pyrolytic, and Combustion Characteristics of Hydrochar Obtained by Hydrothermal Carbonization of Biomass

Ying Gao,[a] Bo Yu,[b] Ke Wu,[a] Qiaoxia Yuan,[a,]* Xianhua Wang,[c,]* and Hanping Chen [c]

Effects of the type of biomass and temperature, with longer residence time, on physicochemical characteristics of hydrochar were investigated. Different carbonization conditions were applied with the goal of producing hydrochars having better physicochemical properties. After the carbonization process, the pyrolysis and combustion behaviors of hydrochar were evaluated. The effect of temperature on the chemical characteristics of hydrochar was obvious. The yield and heating value of hydrochar were high for raw materials. Even though the yield of hydrochar from water hyacinth was low, the morphology of this hydrochar was the best among all biomass samples tested. Hydrochar derived from water hyacinth can be used as a new kind of carbon material, which can improve the utilization of biomass resources. The pyrolysis and combustion behaviors of hydrochar were studied; the corresponding kinetic parameters were determined by thermogravimetric (TG) analysis. With increasing heating rate, the TG and differential thermogravimetric (DTG) curves moved to high temperatures. The combustion of hydrochar had two stages: volatilization and fixed carbon combustion. The activation energy of the wheat straw was 37 kJ/mol, and the activation energy of the water hyacinth was 51 kJ/mol. This data indicated that the combustion of water hyacinth hydrochar was difficult.

Keywords: Hydrothermal carbonation; Hydrochar; Physicochemical; Pyrolytic/combustion kinetics

*Contact information: a: Engineering Technology Academy, Huazhong Agriculture University, Wuhan 430070, PR China; b: School of Management and Engineering, Nanjing University, Nanjing 210013, PR China; c: State Key Laboratory of Coal Combustion, Huazhong University of Science and Technology, Wuhan 430074, PR China; *Corresponding author: qxyuan@mail.hzau.edu.cn ; wxhwhhy@sina.com.*

INTRODUCTION

Rapid global industrialization has increased the demand for petrochemical resources. Because of their rich carbon content, large reserves, wide distribution, low pollution, cheapness, and renewability, biomass resources are potential alternatives to petrochemical resources. Experts estimate that alternative biomass fuels will account for over 40% of the total global energy consumption by 2050 (Nunes *et al*. 2013; Roberts *et al*. 2015), but at present, biomass resources have not been reasonably leveraged. Most biomass is directly burned, and such practices entail low efficiencies and negative environmental consequences (de Koning *et al*. 1985). Developing biomass conversion technologies to produce liquid, solid, or gas fuels diversifies energy resources, reduces dependencies on fossil fuel, and alleviates greenhouse gas emissions. In addition, this field has important significance in sustainably developing energy and safeguarding the environment.

Using currently available technology, biomass can be partially or completely converted into fuels or chemicals through thermo-chemical, biochemical, and other methods. The thermo-chemical method includes thermal pyrolysis and hydrothermal conversion technologies (Kumar and Huhnke 2014). Hydrothermal conversion transforms biomass into low molecular products through a series of physicochemical reactions using subcritical or supercritical conditions of water at certain temperatures and pressures. Hydrothermal conversion of biomass has many potential advantages, as follows:

(1) Water is the reactant and solvent. The biomass does not need to be pre-dried prior to treatment.

(2) Heating under high pressures can reduce the latent heat loss during the process when liquid water is converted to vapor. This improves the thermal efficiency of the process.

(3) At high temperature and pressure, where water is supercritical, water exhibits the nature of an organic solvent, which is advantageous to biomass conversion. Once the reaction is completed, the process is returned to normal temperature and pressure where the water and liquid organic products are separate from one another.

(4) Because water participates in the reaction, the temperature required by the reaction is usually lower than that for thermal pyrolysis (Zhao *et al.* 2014).

(5) Gaseous sulfur oxides and nitrogen oxides are easily solubilized in water, which helps to reduce the emission of harmful gases during the biomass conversion process.

Recent advances in hydrothermal conversion technology allow the direct conversion of biomass into gas, liquid, and carbon products. In particular, hydrothermal carbonization has attracted attention for its promising large-scale application and environmentally friendly advantages. The raw materials used in hydrothermal carbonization method are usually native plants, carbohydrates, and other biomass. Biomass is widely distributed in nature and is a renewable source of carbon. During hydrothermal carbonization, carbonaceous materials with different surface morphologies and various functional groups are prepared from different biomasses and by varying carbonization process parameters.

Unlike the traditional high temperature char method, solid hydrochar is produced by the hydrothermal reaction at 180 to 250 °C, 4 to 24 h, and 1.0 to 4.0 MPa. Hydrothermal conditions are mild, and the process is simple. Through proper control, a large number of carbon-based nano-materials can be synthesized. In addition, many oxygen-containing functional groups are retained on the surface of the hydrochar (Poerschmann *et al.* 2014). The temperature and pressure conditions required are both low and relatively mild. The energy density and quality of hydrochar are similar to peat and lignite (Antonietti and Titirici 2010); thus, hydrochar can be directly burned as a composite solid fuel (Funke and Ziegler 2010). Moreover, char particles of uniform size and good morphology are obtained after hydrothermal crosslinking carbonization of the raw materials. Through synthetic modification, hydrochar can be used in electrodes, fuel cells, and other fields requiring highly efficient and stable nano-scale carbon material (Hu *et al.* 2010).

Due to the wide diversity of biomass, the main three components of cellulose, hemicellulose, and lignin affect the yield and quality of the products. Therefore, it is very important to select appropriate processes and conditions to preserve the energy contained in the biomass during its conversion. Liu and Balasubramanian (2014) compared hydrochar to pyrolytic char and found that the former had higher energy density and the latter had higher energy yield. In addition, hydrochar also had higher thermal efficiency and lower pollutant emissions (Liu and Balasubramanian 2014). Heilmann *et al.* (2010) studied the carbonization of microalgae in a 450 mL autoclave. The heating value of the produced char under the conditions of 200 °C, 0.5 h, and < 2 MPa was 31.58 MJ/Kg, and the production rate was 60 wt.% (Heilmann *et al.* 2010). Nizamuddin *et al.* (2015) performed hydrothermal carbonization of oil palm shell. The cited authors found that the heating value improved up to 22.11 MJ/kg as compared to the heating value of feed palm shell 12.24 MJ/kg, the maximum yield of solid was 60% at 200 °C, 10 min (Nizamuddin *et al.* 2015). Then, they investigated the possible optimum conditions for maximum yield for production of hydrochar through hydrothermal carbonization of palm shell, and the optimized conditions for hydrochar production were found to be 180 °C, 30 min, and 1.60 wt.% (Nizamuddin *et al.* 2016). He *et al.* (2013) examined sludge as a biomass source for hydrochar produced by hydrothermal condition; the investigators studied the fuel characteristics and combustion behavior of the resulting char. The hydrochar was more easily burned than the raw sludge because it had lower activation energy and pre-exponential factor (He *et al*. 2013). Cao *et al.* (2013) studied the physicochemical characteristics of hydrochar produced from bark and sugar beet at various hydrothermal conditions (*i.e*., temperature and residence time). Bark hydrochar was rich in aromatic moieties. Due to the high lignin content of bark, its biochemical oxygen demand (BOD) was higher than that of sugar beet. Long residence time produced a hydrochar rich in aromatic carbon, which led to higher degrees of carbonization (Cao *et al*. 2013).

High value-added heavy oil can be obtained using hydrothermal conversion conducted over a short treatment time. After an extended residence time, hydrochar has a value-added utilization (Poerschmann *et al*. 2014). To obtain high-quality hydrochar, it is necessary to increase liquid oil yield, maximize quality, and adjust reaction time simultaneously. In order to meet the demands of further processing hydrochar into high-added value products, it is necessary to ensure good physicochemical characteristics. Thus, an in-depth study of trends in the physicochemical characteristics of biomass char after the hydrothermal process is important for understanding how to modulate the quality of hydrochar. Gao *et al*. (2012) studied the influence of treatment residence time (5 min to 2 h) on the distribution of hydrothermal products from cellulose, namely, heavy oil, solid residues, and light oil. Low temperature (250 °C) and long residence time (2 h) had an appreciable influence on the physicochemical characteristics of the resulting char (Gao *et al*. 2012).

In this paper, the influence of the type of biomass and temperature with longer residence time on the physicochemical characteristics of hydrochar were investigated. Changes in the physicochemical characteristics of char in the hydrothermal process were examined, revealing the reaction mechanism of the hydrothermal process. The pyrolysis and combustion behaviors of biomass hydrochar were studied with non-isothermal thermogravimetry with the determination of kinetic parameters and the application of mathematical modeling. The results of this work provide reference values for optimizing the hydrothermal carbonization reaction conditions of biomass and realizing the high-value utilization of hydrochar.

EXPERIMENTAL

Materials

Wheat straw, cotton stem, rice straw, pine sawdust, and water hyacinth were selected as raw materials for experimentation. The materials were crushed and sieved with an 80-mesh screen; materials passing through the 80-mesh screen were dried at 55 °C for 8 h and then sealed in a drying oven.

Hydrothermal Carbonization: Procedure and Analysis

Hydrothermal carbonization was performed in a CWYF-series high-temperature and high-pressure batch reactor produced by Haian County Petroleum Scientific Research Instrument Co., Ltd (Nantong, China). The reactor was constructed from 316 L stainless steel and had a volume of 500 mL. The design temperature and pressure of the reactor are 600 °C and 40 MPa, respectively. The reactor was heated using an electric stove. The temperature was controlled using a K-type thermocouple to within ± 5 °C of the set-point value. Raw materials (4 g) and deionized water (110 g) were placed into the reactor. The reactor was sealed and flushed with nitrogen to expel the air. Then, the reactor's exhaust valve was closed. When the pressure gauge reached 4 MPa, the inlet valve was closed. After 10 min, the air tightness of the reactor was evaluated. When this requirement was met, the exhaust valve was opened to reduce the pressure to 0 MPa (gage). Afterwards, the reactor temperature was set, and its stirring speed was set to 600 rpm while heating. After the prescribed experimental conditions, the reactor was cooled by feeding tap water into the internal U-shape ring and by blowing air onto the reactor with an external fan. When the temperature of the cooling reactor reached 90 °C, the reactor's exhaust valve was opened. Because the error of each result was within 1%, the experimental runs were replicated three times, and the results reported are the average values.

The reactor was opened after cooling. The stirrer and pipelines were cleaned with deionized water. The reaction products were separated into liquid and solid products, as shown in Fig. 1.

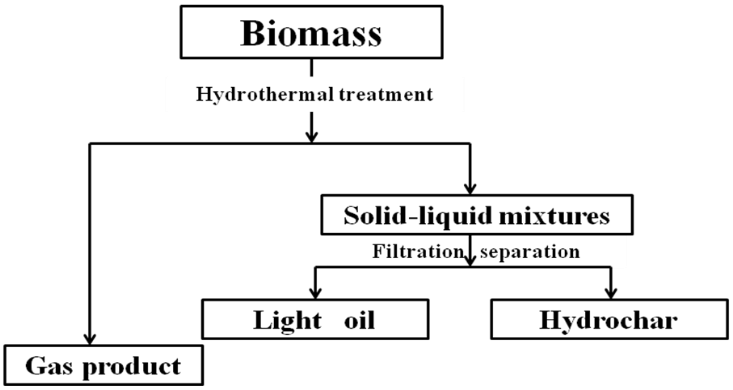

Fig. 1. Product separation after hydrothermal carbonation

The liquid product is defined as light oil. The solid product was dried at 105 °C until it reached constant mass; the dried solid product, defined as hydrochar, was then sealed. The hydrochar yield, higher heating value (HHV) as determined by the method of Sheng and Azevedo (2005), and hydrochar energy yield were calculated by Eqs. (1), (2) and (3), respectively:

$$\text{Hydrochar Yield }(\text{wt. \%}) = \left(\frac{\text{weight of hydrochar}}{\text{weight of raw material}}\right)\times 100 \tag{1}$$

$$\text{HHV }(\text{MJ/kg}) = 0.3383\times \text{C} + 1.422\times\left(\text{H} - \frac{\text{O}}{8}\right) \tag{2}$$

$$\text{Energy Yield }(\text{wt. \%}) = (\text{Hydrochar Yield})\times\left(\frac{\text{HHV}_{\text{hydrochar}}}{\text{HHV}_{\text{raw material}}}\right)\times 100 \tag{3}$$

An Agilent 7890A/5975c gas chromatography mass spectrometry (GC-MS) instrument (Santa Clara, CA, USA) was used to analyze the composition of the liquid product. It was difficult to detect the organics in the light oil due to its high moisture content. Thus, diethyl ether extractions of the light oil were conducted to extract the organics. A total of 15 mL of light oil was placed into a 250-mL separatory funnel, and 100 mL of ether was added. The light oil was extracted to obtain a light yellow organic liquid layer phase. The collected light yellow liquid was added to a 250-mL rotary evaporation flask. The sample volume was reduced using a rotary evaporator to yield a concentrated oil, and the oily residue was analyzed with GC-MS using a HP-5 weak-polar capillary column. The GC-MS temperature profile that was as follows: 45 °C constant temperature for 5 min, heating to 250 °C for 5 °C/min, and 250 °C constant temperature for 10 min.

The elemental analysis of the raw materials were conducted using a Series II CNHS/O 2400 elemental analyzer (PerkinElmer, Akron, OH, USA). Thermogravimetric analysis (TGA) was conducted using a TGA-2000 analyzer (Navas Instruments, Conway, SC, USA). The samples were placed into TGA vessels, which were transferred to the low-temperature furnace. The dried samples were placed into the high-temperature furnace, which was filled with nitrogen and heated for 7 min in advance. Next, oxygen was introduced into the furnace, and the samples were ashed to a constant weight. The weight losses were determined by electronic balance to obtain moisture, volatile materials, ash, and fixed carbon content in the samples. An ANKOM 2000 fiber analyzer (Macedon, NY, USA) was used to measure the biomass contents of three components of. A Quanta 200 scanning electron microscope (SEM; FEI, Eindhoven, Netherlands), was employed to characterize the microstructure of the hydrochar. Fourier transform infrared (FTIR) spectroscopy was performed on a Vertex 70 instrument (Bruker, Karlsruhe, Germany). This scanning analysis explored the influence of the hydrothermal treatment on the functional groups of hydrochar.

Pyrolysis and Combustion Analysis

Wheat straw and water hyacinth were hydrothermally carbonized at 240 °C for 4 h. Each raw material was crushed and sieved through 80- to 150-mesh screens. The carrier gas for pyrolysis was high purity nitrogen (99.9999%) used at a flow rate of 50 mL/min. Samples (5 mg) were heated to 105 °C at heating rates of 5, 10, 20, and 50 °C/min and then incubated for 5 min to completely dry the samples. Finally, the samples were heated to 900 °C until pyrolysis was complete. Combustion analysis was also conducted on hydrothermally carbonized wheat straw and water hyacinth. Samples (5 mg) were heated to 105 °C at 10 °C/min and then incubated for 5 min to completely dry the samples. Finally, the dried samples were heated to 600 °C until combustion ended.

Kinetic Analysis

Because of its simplicity, convenience, rapidness, and accuracy, thermal gravimetric analysis (TGA) is an important tool for studying thermal decomposition in biomass. There has been little research on obtaining pyrolysis and combustion characteristics from TGA data. In this paper, non-isothermal thermogravimetry was used to explore hydrochar pyrolysis and combustion to obtain the relevant weight loss law and to determine kinetic parameters of the mathematical rate model. Based on the kinetic expression of a heterogeneous reaction, the generalized kinetic equations were as follows,

$$\frac{d\alpha}{dt} = k(T)f(\alpha) \tag{4}$$

$$\alpha = \frac{m_0 - m_t}{m_0 - m_\infty} \tag{5}$$

$$g(\alpha) = kt \tag{6}$$

where α was the fractional of weight loss of the sample at time t; m_0, m_t and m_∞ were the initial mass, the mass at time t and the residual mass, respectively, of the sample. It was assumed that the rate constant of Eq. 4, which is a function of reaction temperature, conformed to Arrhenius' law (*i.e.*, $k = A \cdot \exp(-E_a/RT)$). Thus, Eqs. 4 and 6 can be transformed into,

$$\frac{d\alpha}{dt} = A\exp\left(-\frac{E_a}{RT}\right)f(\alpha) \tag{7}$$

$$g(\alpha) = A\exp\left(-\frac{E_a}{RT}\right)t \tag{8}$$

where $f(\alpha)$ and $g(\alpha)$ were the reaction mechanism functions, A was the pre-exponential factor, E_a was the energy of activation of the reaction, R was the universal gas constant (8.314×10^{-3} kJ/mol•K), and T was the thermodynamic temperature. Based on $\beta = dT/dt$, the kinetic equation under the non-isothermal condition was as follows:

$$g(\alpha) = \frac{A}{\beta}\int_0^T \exp\left(\frac{E_a}{T}\right)dT \tag{9}$$

Usually, differentiation is to make analysis based on the DTG curve and integration is to make analysis in the integral form based on TG curve. Because integration does not consider the error caused by derivative calculation in the calculation process, it is adopted in the paper for analysis. If $E_a/(RT)$ is replaced by x and converted into the range of integration, Eq. 9 becomes：

$$g(\alpha) = \frac{AE_a}{RT}\int_x^\infty \frac{\exp(-x)}{x^2}dx \tag{10}$$

Equation 10 can be expressed as $g(\alpha) = \frac{AE_a}{RT}p(x)$, $p(x) = \int_x^\infty \frac{\exp(-x)}{x^2}dx$. The integral of p(x) was approximated and the natural logarithm of both sides was taken to yield Eq. (11), as proposed by Coats and Redfern (1964):

$$\ln \frac{g(\alpha)}{T^2} = \ln \left[\frac{AR}{\beta E_a} \left(1 - \frac{2RT}{E_a} \right) \right] - \frac{E_a}{RT} \tag{11}$$

For the temperature range where E_a»2RT, so $1 - \frac{2RT}{E_a} \approx 1$. Inserting this approximation into Eq. 11 yields the expression:

$$\ln \frac{g(\alpha)}{T^2} = \ln \left[\frac{AR}{\beta E_a} \right] - \frac{E_a}{RT} \tag{12}$$

A graph of $\ln \frac{g(\alpha)}{T^2}$ versus $\frac{1}{T}$ should yield a straight line. E_a and A can be calculated from the slope and intercept of this line.

In the pyrolysis/combustion reaction process, using random nucleation and its subsequent growth, n = 1 was adopted. The integral form can be expressed as follows (Turmanova *et al*. 2008):

$$g(\alpha) = -\ln(1-\alpha) \tag{13}$$

The kinetic parameters of different biomass were calculated with Eq. 14. The pyrolysis/combustion reaction process was divided into several stages, and the obtained pyrolytic kinetic parameters were the ones of a given temperature range. In order to describe the overall reaction kinetic parameters of reaction, Cuming (1984) suggested a weighted average activation energy (E_m), specifically expressed as,

$$E_m = F_1 \times E_1 + F_2 \times E_2 + \cdots + F_n \times E_n \tag{14}$$

where E_1 to E_n refers to the average apparent activation energy of each stage, and F_1 to F_n refers to the relative weight loss.

RESULTS AND DISCUSSION

Feedstock Characterization

The main characteristics of the biomass feedstocks are shown in Table 1. The volatile contents and O content were high in straw materials and pine sawdust; the ash content was the lowest in pine sawdust (0.20 wt.%), which resulted in the highest heating value of 18.16 MJ/kg. The contents of N and S were low in the agricultural straws and pine sawdust. However, the O and volatile contents were low in water hyacinth; its N, ash, and S contents were noticeably higher than the other four biomass materials, which resulted in its low heating value.

Compared with other biomasses, water hyacinth contained low cellulose and lignin levels. Besides cellulose, hemicellulose, and lignin, water hyacinth contained some fat and crude protein.

Table 1. Main Characteristics of the Biomasses (wt.%)

Sample		Wheat Straw	Cotton Stem	Rice Straw	Water Hyacinth	Pine Sawdust
Elemental Analysis (wt. %, dry basis)	N	0.55	1.15	0.86	2.03	0.10
	C	40.36	45.22	37.52	29.75	51.01
	S	0.27	0.34	0.14	0.33	0.02
	O*	52.87	46.94	42.78	22.68	42.90
	H	5.95	6.34	5.92	5.41	6.00
Proximate Analysis (wt. %, air dry basis)	M	4.38	5.10	5.04	5.69	15.30
	V	68.52	72.98	82.12	49.92	70.4
	A	12.91	3.09	7.74	38.11	0.2
	FC	14.20	16.73	5.10	6.28	14.19
	HHV (MJ/kg)	12.72	15.97	13.51	13.73	18.16
Chemical Analysis (wt. %)	Cellulose	40.4	46.20	37.50	23.50	55.30
	Hemicelluloses	25.6	18.70	32.80	33.6	10.10
	Lignin	22.3	25.4	16.00	8.60	27.20

M: moisture content; V: volatile materials; A: ash; FC: fixed carbon.
*: The oxygen (O) content was determined by difference.

Effect of Different Biomasses

Figure 2 shows the energy yield and mass yield distribution of hydrochar of various biomasses. The mass yield of different biomasses were ranked from highest to lowest as follows: cotton stem> pine sawdust > rice straw > water hyacinth. The high energy and mass yields for cotton stems and pine sawdust were attributed to their high contents of cellulose and lignin and their low content of hemicellulose.

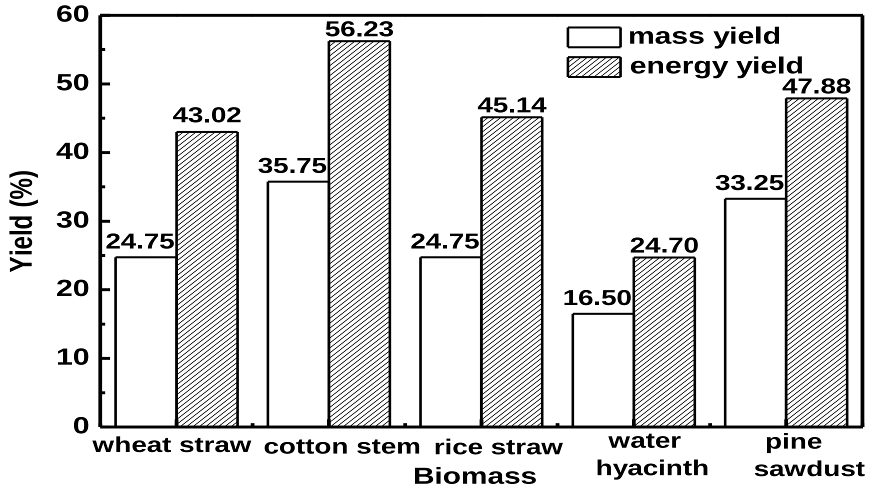

Fig. 2. Energy yield and mass yield of hydrochar obtained from different biomasses

As previously noted (Yang *et al*. 2007; Kumar *et al*. 2011; Gao *et al*. 2013), char is formed through the condensation and polymerization of compounds produced by the oxidation of monosaccharides; monosaccharides are produced from the hydrolysis of cellulose and hemicelluloses. Due to the low reaction temperatures employed, lignin can only be hydrolyzed partially, so the lignin content also affects the yield of char. The ash content may also affect the yield. Table 1 shows that the ash contents in cotton stem and pine sawdust were both low. The hydrochar mass yields of wheat straw and rice straw were similar to one another, whereas that of water hyacinth was the lowest, which was attributed to the low lignin and carbohydrate contents and high ash content. The hydrochar energy yields from different biomasses ranged between 24% and 57%, whereas the hydrochar mass yields ranged between 16% and 36%. The energy yield of cotton stem was the highest (56.23%), while that of water hyacinth was the lowest (24.7%).

Figure 3(a) shows the FTIR spectra of the five biomasses. The chemical compositions of the biomasses mainly contained different oxygen functional groups, including ether (OH (3400 to 3200 cm^{-1})), aromatics (C = O (1765 to 1715 cm^{-1}), and alkanes (C-O (1050 cm^{-1}, 1270 cm^{-1}). Ketone (3000 to 2800 cm^{-1}) and alcohol (900 to 700 cm^{-1}) were also present. Due to the different cellulose, hemicellulose, and lignin contents in straw, wood and aquatic plants, there were different IR absorption properties. Figure 3(b) shows the infrared spectra of hydrochar of different biomass materials. According to the figure, hydrochar obtained from the five biomass materials had a weak absorption peak of water at 3423 cm^{-1}, an absorption peak of an alkane at 3000 to 2750 cm^{-1}, an absorption peak of an ester at 1900 to 1500 cm^{-1}, and an absorption peak for alcohol and other small compounds at 1500 to 900 cm^{-1}. Compared with Figure 3(a), the chemical structure of hydrochar after the hydrothermal treatment had obvious changes, including the weakening of the OH peak and the reduction of IR absorption from C-H bond (alkene). Usually, the rupture of C-H bonds releases the gaseous hydrocarbons CH_4, C_2H_6, and C_2H_4, which reduces the H content in the hydrochar. In addition, as C=C, C-O and C-H bonds in the hydrochar were fractured and reformed as volatile gases, the IR absorption peaks of these groups were reduced. According to Table 3, as the volatile content in the hydrochar decreased, the heating value increased compared with the original sample. The absorption peak of hydrochar from cotton stem and pine sawdust was strong at 2925 cm^{-1} and weak at 1500 to 900 cm^{-1}, which was correlated to the high heating value for these materials. This result was mainly attributed to the complete hydrolysis of cellulose. The absorption peak of hydrochar from wheat straw was the weakest at 1500 to 900 cm^{-1}.

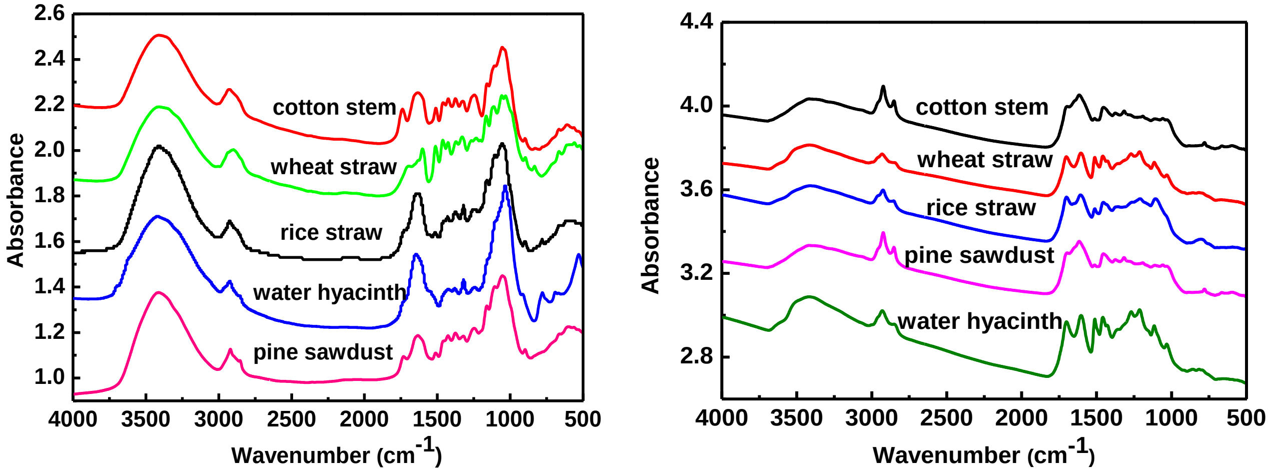

(a) (b)

Fig. 3. FTIR spectra for (a) different biomasses and (b) hydrochar obtained from different biomasses at 240 °C and 4 h

Results of elemental and proximate analyses of hydrochar from different biomasses are shown in Table 2. The hydrochar mainly contained C, H, and O, as well as a small amount of N and S; this observation is consistent with the previous infrared results, which indicated that hydrochar was rich in oxygen functional groups after hydrothermal conversion. The C content in hydrochar from different biomasses increased, while the O, H, and volatile contents decreased compared with the original samples. While the C content in hydrochar of pine sawdust was 68.65 wt.%, the ash content was 4.02 wt.%, and the volatile content was as high as 58.39%. The C content in water hyacinth hydrochar was the lowest (46.51 wt.%); its ash content was 31.11 wt.%. This result was attributed to the ash and volatile contents, which caused the low heating value of water hyacinth hydrochar. The hydrochar heating values obtained from different biomass materials were ranked from highest to lowest: pine sawdust > cotton stem> rice straw > wheat straw > water hyacinth.

Table 2. Elemental and Proximate Analyses of the Hydrochar from Different Biomasses (wt. %)

	Wheat Straw	Cotton Stem	Rice Straw	Water Hyacinth	Pine Sawdust
Elemental Analysis (wt. %, dry basis)					
C	58.30	65.23	63.07	46.51	68.65
H	4.17	4.41	4.53	5.04	4.76
N	0.99	0.82	2.38	3.70	0.77
S	0.09	0.08	0.18	0.41	0.21
O *	19.91	18.14	17.71	13.23	21.59
Proximate Analysis (wt. %, air dry basis)					
M	1.30	0.25	0.85	0.86	0.73
V	49.44	53.15	53.58	45.78	58.39
A	16.54	11.32	12.12	31.11	4.02
FC	32.72	35.28	33.44	14.20	36.85
HHV (MJ/Kg）	22.11	25.12	24.64	20.55	26.15

M: moisture content; V: volatile materials; A: ash; FC: fixed carbon.
*：The oxygen (O) content was determined by difference.

SEM analysis showed the surface structure properties of hydrochar samples (Fig. 4). Under the hydrothermal conditions of 240 °C and 4 h, the hydrochar from wheat straw was flocculent in appearance. Its surface structure was loose. Cotton stem hydrochar was mainly layered with a small number of pores; the surface structures of rice straw and sawdust hydrochars were similar without a layered structure. Their hydrochar surfaces were mainly granular. Water hyacinth hydrochar presented carbon microstructure. The formation of microsphere structural elements was clearly visible. Carbon microspheres had diameters approaching the nanometer level.

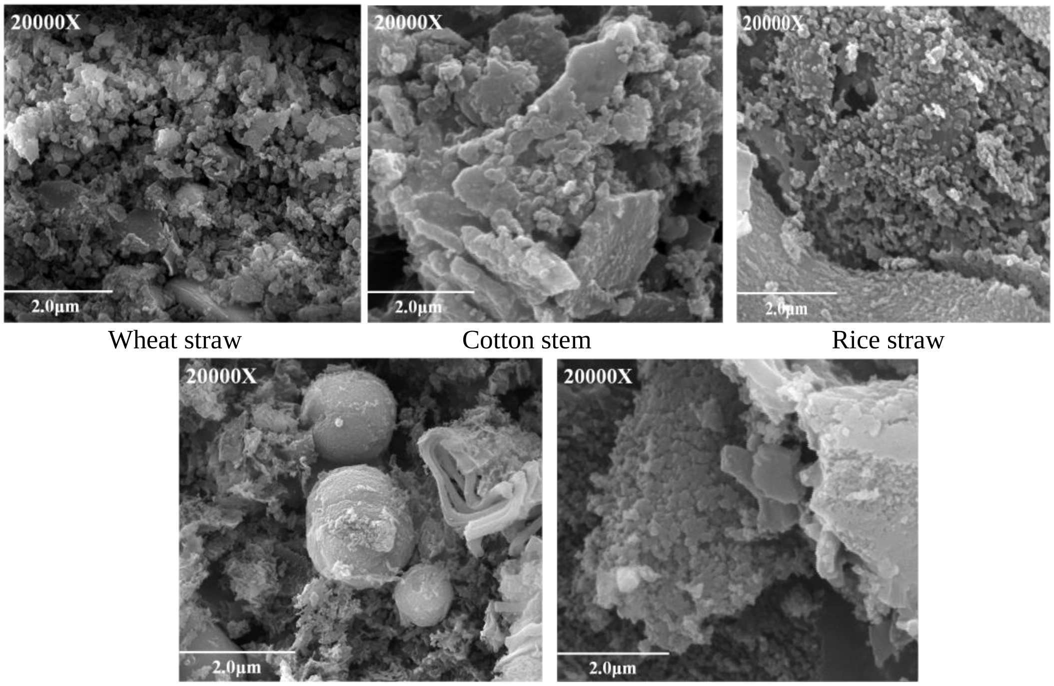

Wheat straw Cotton stem Rice straw

Water hyacinth Pine sawdust

Fig. 4. SEM images of obtained hydrochar from different biomasses

The light oil products of wheat straw, cotton stem, rice straw, pine straw, and water hyacinth were analyzed (Table 3) in order to further understand the formation of hydrochar in the hydrothermal process.

Table 3. GC-MS Analysis Results of the Light Oil Products from Different Biomasses

Compound	Biomasses				
	Wheat Straw	Cotton Stem	Rice Straw	Water Hyacinth	Pine Sawdust
Furfural	23.5	21.31	18.04	0.73	22.83
Phenol	1.44	0.84	3.31	1.35	0.94
5-Hydroxymethylfurfural	3.55	3.13	0.45	—	3.99
Guaiacol	6.06	10.63	9.48	7.98	11.27
2,6-Dimethoxyphenol	5.42	10.63	7.38	5.71	10.99
1,2-Benzenedicarboxylicacid, 1-(2-ethylhexyl) ester	13.3	2.4	6.16	25.1	4.33
Vanillin	2.37	2.93	1.36	—	2.07
Hydroquinone	1.86	2.65	1.81	0.2	1.96
Acetosyringone	2.69	0.94	4.82	0.51	1.02
4-Ethyl guaiacol	2.79	2.47	3.09	2.96	2.91
3-Hydroxypyridine	—	—	0.33	10.12	—
Acetovanillone	1.37	1.33	2.67	4.27	1.49

Twelve functional groups were detected by GC-MS analysis, including phenol, ester, ketone, and aldehyde. The content of furfural in the light oil product of water hyacinth was only 0.73 wt.%, whereas it was much higher in the other biomasses (18 to

23 wt.%). 5-Hydroxymethylfurfural and vanillin were not detected in water hyacinth. In addition, the ester compound content in water hyacinth was 25 wt.%, which was appreciably higher than in other biomasses. The ketone and phenolic contents in water hyacinth were similar to those in straw materials, being about 18 wt.% and 8 wt.%, respectively; this indicated that these materials had considerable differences in hydrochar characteristics and light oil compositions after the hydrothermal treatment. This was mainly attributed to volatile contents in biomasses being rapidly separated from the solid reaction system at the initial stage of hydrothermal carbonization. Among the three main components of lignocellulose, hemicelluloses were the most easily degraded, and their rapid degradation occurred during the initial stage of hydrothermal carbonization. The hemicellulose content in water hyacinth was higher than that of cellulose and lignin, which led to its low aldehyde content. As the reaction time continued, the degradation of hemicelluloses was essentially complete, whereas the degradation of cellulose was slow throughout hydrothermal carbonization (Yu *et al*. 2007; Peterson *et al*. 2008). In addition, the furfural content in the light oil had no great influence on the formation of carbon microspheres, which was mainly affected by phenolic and ketone compounds (Kang *et al*. 2012; Xiao *et al*. 2012).

Effect of Hydrothermal Temperature

The influence of reaction temperature on the yield of hydrochar from wheat straw was studied with a reaction time of 4 h and varying temperature (200 to 280 °C). The energy and mass yields of the hydrochar at different hydrothermal temperatures are shown in Fig. 5.

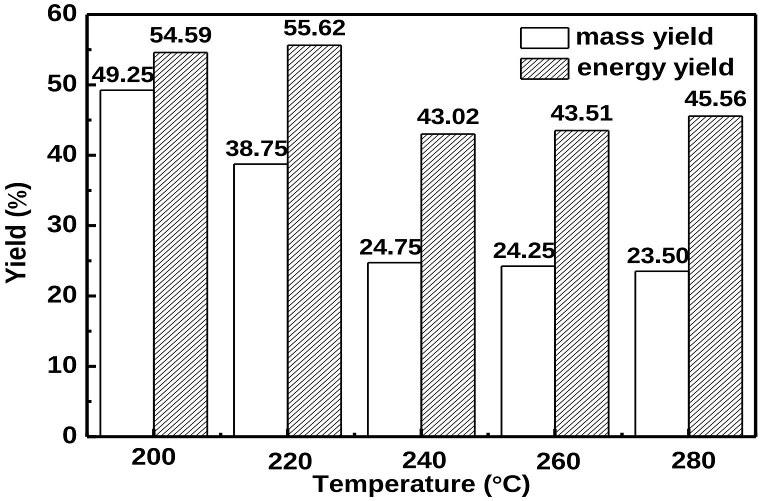

Fig. 5. Energy yield and mass yield of wheat straw hydrochar produced at different temperatures

With increasing reaction temperature, the energy yield of the hydrochar produced by the carbonization process increased from 54.59% at 200 °C to the maximum of 55.62% at 220 °C; higher carbonization temperatures caused the energy yield to decrease from the maximum value. When the temperature was higher than 240 °C, the energy yield increased gradually, and the mass yield changed slowly. In addition, with increasing hydrothermal temperature (240 °C to 280 °C), the difference between mass yield and energy yield became larger gradually. This was mainly due to the great increase in energy density in wheat straw after the hydrothermal treatment. When the temperature rose to

280 °C in the hydrothermal process, the energy yield was reduced. The volatile materials produced during the carbonization process resulted in hydrochar mass loss and subsequent energy loss; however, during hydrothermal carbonization, the degradation of lignocellulose produced small pieces of hydrochar that were released as inert gas, leading to further energy loss. Thus, 220 °C was the optimum reaction temperature for hydrochar, at which the energy yield was at its maximum value.

The FTIR spectra of hydrochars produced at different hydrothermal temperatures are shown in Fig. 6. The infrared spectra of hydrochars were similar to that of wheat straw. The absorption peak of lignin was present, indicating that hydrochar had a similar molecular structure to lignin. At 200 °C and 220 °C, there were strong absorption peaks at 1060 and 1160 cm^{-1}. These peaks corresponded to C-O-C stretching vibration and C-O stretching in of cellulose and hemicelluloses, which indicated that the wheat straw had not hydrolyzed completely. When the reaction temperature was 240 °C, the C-O-C, C-O, and C-H absorption peaks were reduced, which indicated that CO_2 and gaseous hydrocarbons were quickly released. There were absorption peaks for olefins at 1680 and 1580 cm^{-1} and an absorption peak of an ether bond at 1250 cm^{-1}, reflecting that aromatic rings were recombined into new compounds at higher reaction temperatures. Above 260 °C, the intensity of OH, C-O, and C-H peaks for hydrochar reduced sharply. Thus, the hydrothermal decomposition reaction was at 240 to 260 °C because the hydrothermal degradation process of wheat straw consisted of hydrolysis and pyrolysis. In the low-temperature stage, it underwent appreciable hydrolysis. In the high-temperature stage, it underwent pyrolysis. Sugars, alkanes, esters, and acids produced by hydrolysis at lower temperatures were converted to ketones, phenols, aldehydes, benzodiazepines, and heterocyclic compounds by condensation and cracking reactions at higher temperatures. Hydrochar had absorption peaks of lignin at 1211, 1446, and 1506 cm^{-1} and strong absorption peaks of condensation polymer at 1602 and 1703 cm^{-1}, indicating that hydrochar was mainly composed of lignin and of condensation polymer in the hydrothermal conversion process.

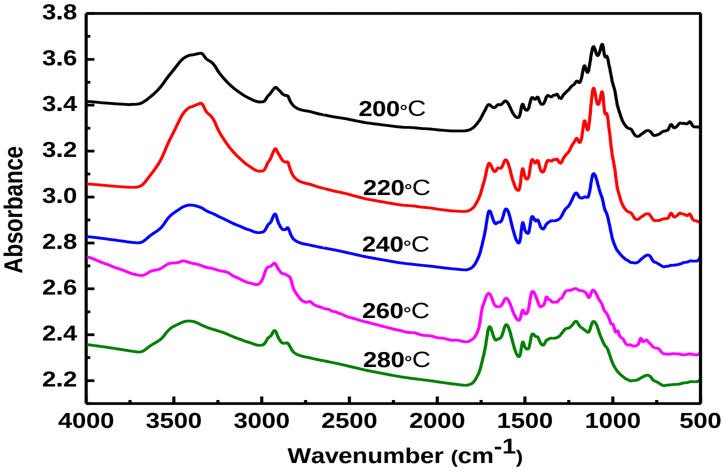

Fig. 6. FTIR spectra of wheat straw hydrochar from different temperature

The characteristics of wheat straw hydrochar are shown in Table 4. The C content in hydrochar was greatly reduced when compared with that in the raw material. This was because the decarboxylation reaction promoted the formation of CO and CO_2 during the carbonization process. Due to the dehydration reaction between hydrogen free-radicals and oxygen atoms in the hydrothermal carbonization process, the O content in hydrochar obtained from the aqueous solution was much lower than raw wheat straw. With the increase of temperature from 240 °C to 260 °C and the separation of volatile materials, the O content was obviously reduced, which indicated that the hydrothermal pyrolysis of the oxygen functional groups in wheat straw occurred during this temperature range. This result was consistent with the FTIR analysis. The C and H contents in hydrochar increased with rising temperature. The C content was 47.73 wt.% at 200 °C and rose to 62.31 wt.% at 280 °C. The H content did not appreciably change. Higher hydrothermal temperature produced a higher the degree of carbonization. Due to increasing C content, the fixed C content of the product increased extensively. However, the volatile content decreased, and the heating value increased. At 280 °C, the HHV was 24.66 MJ/Kg. The N and S contents in the raw wheat straw sample were very low. When the hydrothermal temperature increased, the S and N contents in hydrochar did not change appreciably. The high N content in hydrochar was due to the high protein component in wheat straw, which is the N-containing organic compound.

Table 4. Characteristics of Wheat Straw Hydrochar from Different Temperatures

	Wheat Straw	200 °C	220 °C	240 °C	260 °C	280 °C
Elemental Analysis (wt.%, dry basis)						
C	40.36	47.73	52.01	58.30	61.21	62.31
H	5.95	3.01	4.00	4.03	4.10	4.17
N	0.55	0.64	0.71	0.99	1.09	1.78
S	0.27	0.07	0.10	0.09	0.76	0.09
O	52.87	35.56	29.07	19.91	20.14	12.08
Proximate Analysis (wt.%, air dry basis)						
M	4.38	1.26	1.22	1.30	1.22	1.18
V	68.52	65.10	58.83	49.44	46.68	33.09
A	12.91	12.96	14.01	16.54	17.6	19.71
FC	14.2	20.68	25.94	32.72	34.50	46.02
HHV(MJ/Kg）	12.72	14.1	18.26	22.11	22.82	24.66

SEM was used to analyze hydrochar under different temperatures (Fig. 7). When the temperature was 200 °C, the hydrochar surface was fractured, with layered pores and a small amount of carbon microspheres that had diameters of about 1 μm.

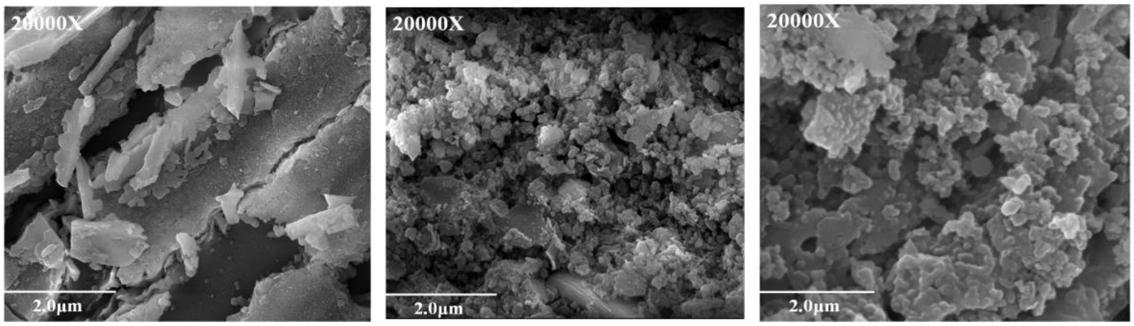

200 °C 240 °C 280 °C

Fig. 7. SEM images of wheat straw hydrochar from different temperature

Due to the low temperature, the hydrolysis reaction was incomplete, and the organic content of the liquid product was low, leading to the slow growth of microspheres. When the temperature rose to 240 °C, cellulose hydrolysis was complete. Phenols and ketones increased, creating more microspheres and more developed and looser pores on the hydrochar surface. At 280°C, microspheres on the hydrochar surface were more evident, but they were adhered to one other.

The GC-MS analysis of light oil (Table 5) showed that the furfural content was highest at 200 °C (72.88 wt.%). With higher temperatures, aldehydes in the light oil gradually decreased, and ketone and phenolic compounds increased. Guaiacol increased from 2.59 wt.% at 200 °C to 11.63 wt.% at 280 °C. Hydroquinone was not detected at 200 °C, and its content was 9.22wt. % at 280 °C. Despite the increase, the content of ketones did not change (2 wt.%). The ester compounds reached a maximum value (13.3 wt.%) at 240 °C. Wheat straw contained lignin, cellulose, and hemicelluloses. Due to the low-temperature hydrolysis reaction of the cellulose and hemicelluloses degraded polysaccharide in it (Gao *et al*. 2012). Polysaccharides were further degraded into monosaccharide-reducing sugars. Peterson *et al.* proposed that increasing the temperature rapidly degrades reducing sugars and promotes further hydrolysis to produce acids and aldehydes. The high reaction temperature is beneficial to promoting polysaccharide as the intermediate product of wheat straw to be converted into small molecular compounds, like organic acids, aldehydes, and alcohols. Thus, the high reaction temperature reduced the aldehyde content and increased the phenolic and organic acid compounds (Gao *et al*. 2013).

Table 5. GC-MS Analysis Results of the Light Oil Products from Wheat Straw

Compound	200 °C	240 °C	280 °C
Furfural	72.88	23.50	11.07
Phenol	0.07	1.44	4.80
5-Hydroxymethylfurfural	4.59	3.55	—
Guaiacol	2.59	6.06	11.63
2,6-Dimethoxyphenol	2.14	5.42	8.26
1,2-Benzenedicarboxylicacid, 1-(2-ethylhexyl) ester	3.24	13.3	2.13
2- Methylacrylic acid	—	5.19	8.24
Vanillin	1.98	2.37	0.66
Hydroquinone	—	1.86	9.22
Acetosyringone	0.55	2.69	2.34
4- Ethyl phenol	0.23	0.73	1.14
4-Ethyl guaiacol	—	2.79	3.82

Kinetics of Hydrochar Formation

Pyrolytic characteristics

Figure 8 presents the TG and DTG curves of wheat straw and water hyacinth hydrochars of at 240 °C and 4 h for the four different heating rates (*i.e.*, 5, 10, 20, and 50 °C/min). The maximum mass loss rate of the hydrochar corresponded to 420 °C for wheat straw and 400 °C for water hyacinth. The pyrolysis of wheat straw and water hyacinth occurred at 200 and 500 °C, which was mainly due to the separation of volatile materials. The separation of volatile materials in the wheat straw hydrochar was divided into two stages. In the first stage from 150 to 350 °C, a small amount of volatile material was separated, primarily hemicelluloses and cellulose, which had not completely reacted (Harun *et al*. 2011). In the second stage at 350 to 500 °C, the weight loss rate was high, and the volatile materials were rapidly separated. The loss of volatile materials was mainly concentrated at the high-temperature area because the hydrochar existed in two forms: a polymerized phenolic hydrochar and the isomerized aromatic hydrochar. These forms were separated at high reaction temperatures. At 500 °C, the hydrochar weight loss rate was about 90%. Later, the weight loss rate decreased due to further cleavage and aromatic conversion of C-H bonds and C-O bonds. The separation of volatile materials in the water hyacinth hydrochar occurred from 200 to 500 °C, which indicated that cellulose and hemicelluloses were completely hydrolyzed during the hydrothermal conversion of water hyacinth.

With the higher heating rate, the hydrochar weight loss curve moved towards the high-temperature range, and the initial pyrolysis temperature, weight loss peak temperature, and pyrolysis termination temperature of all samples increased. At the same time, the weight loss amount in the same temperature range decreased slightly, and the DTG peak moved to the high-temperature range. At the same temperature, the hydrochar initially underwent the first-order pyrolysis. When the pyrolysis temperature was relatively low, hemicelluloses and cellulose were pyrolyzed. At the low heating rate, hydrochar was evenly heated for a long time, leading to the complete loss of volatile organics and the slight loss of the solid residuals. With the high heating rate, the required pyrolysis temperature was also high, which inhibited the separation of volatile materials to a certain degree. The hydrochar components reacted with one other to generate a material that was more resistant to thermal decomposing. As a result, the maximum mass loss peak occurred at a higher temperature.

In addition, the volatile materials content in the wheat straw hydrochar and its maximum pyrolysis rate were significantly higher than water hyacinth hydrochar. This result was due to the different volatile and ash contents in the hydrochar and also due to the residual cellulose and lignin in the hydrochar. According to the kinetic parameters listed in Table 6, as the heating rate increased, the activation energy of hydrochar at two weight loss stages increased. Thus, the heating rate had a positive and a negative effect on pyrolysis.

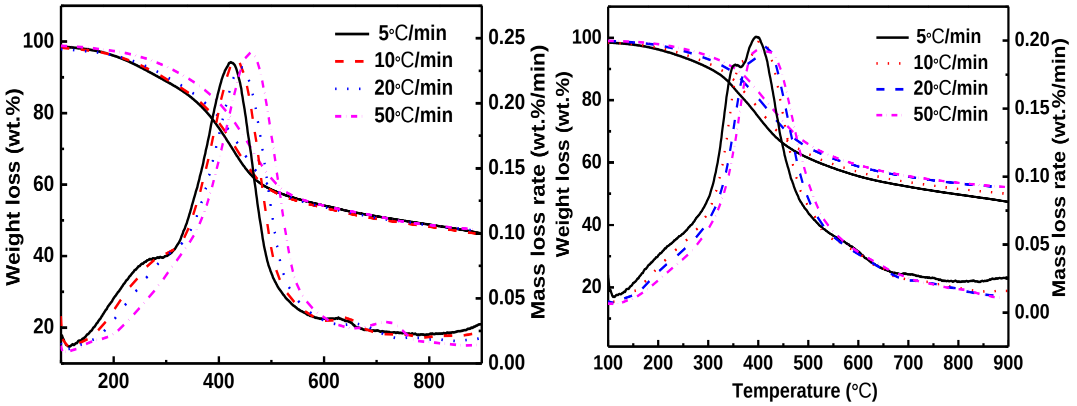

(a) wheat straw (b) water hyacinth

Fig. 8. TG and DTG curves of (a) wheat straw and (b) water hyacinth hydrochar pyrolysis at different heating rates

A higher heating rate required less time for pyrolysis, which was conducive for pyrolysis. However, the high heating rate caused a temperature gradient in the samples due to the heat transfer temperature differential, which led to a heating lag phenomenon in the samples and a shift of the TG curve to higher temperatures. The heat transfer lag phenomenon was related to the heat transfer characteristics of the samples and the sample particle sizes.

Table 6. Kinetics Properties of Wheat Straw and Water Hyacinth Hydrochar Pyrolysis

Biomass	Heating Rate (°C/min)	Temperature Range (°C)	n	Weight Loss (wt%)	E_a (kJ/mol)	A (s^{-1})	R	E_m (kJ/mol)
Wheat Straw	5	200-320	1	8.86	15.79	0.1416	0.9965	21.98
		320-500	1	28.62	23.89	1.0019	0.9869	
	10	200-320	1	8.4	15.48	0.2442	0.9994	22.93
		320-500	1	29.53	25.05	2.5	0.9883	
	20	200-350	1	7.68	14.39	0.3579	0.9971	24.44
		350-520	1	31.10	26.92	7.2	0.9910	
	50	200-360	1	9.49	16.48	1.2	0.9904	29.36
		360-540	1	30.94	33.31	60.2	0.9928	
Water Hyacinth	5	200-340	1	10.35	14.65	0.1	0.9943	22.63
		340-450	1	19.79	26.81	2.12	0.9942	
	10	200-350	1	10.21	15.57	0.24	0.9913	25.46
		350-460	1	20.06	30.50	9.52	0.9954	
	20	200-360	1	10.09	17.63	0.75	0.9944	27.88
		360-480	1	20.77	32.86	28.6	0.9935	
	50	200-360	1	8.59	17.80	1.7	0.9930	30.55
		360-500	1	23.65	35.18	1.0×10^2	0.9900	

Note. R: sample correlation coefficient

Combustion characteristics

The combustion TG and DTG curves of wheat straw and water hyacinth hydrochars are shown in Fig. 9.

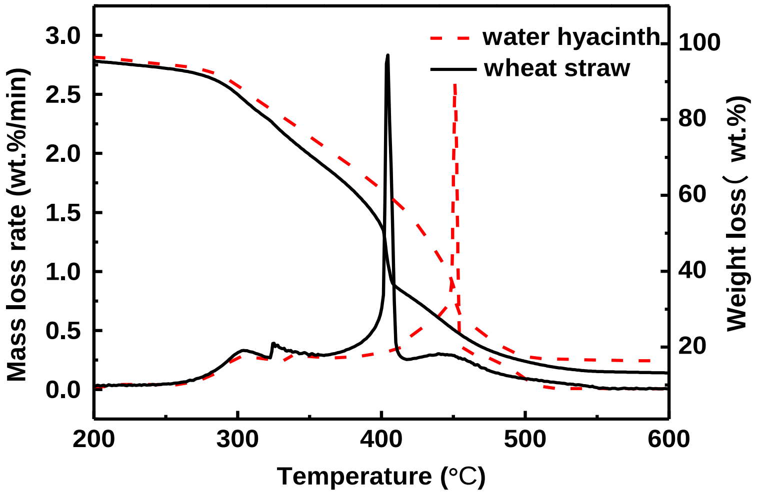

Fig. 9. TG and DTG curves for combustion profiles of wheat straw and water hyacinth hydrochar

The combustion of hydrochar chiefly followed a two-stage process. During the first stage from 270 to 360 °C, weight loss was slow with a rate of only 20.8%. The DTG curve had a small peak, which was mainly attributable to the loss of volatile materials and combustion. After being heated, the volatile materials in hydrochar first reached the ignition temperature and burned, which accelerated the combustion of more volatile materials. This was due to hemicelluloses and cellulose decomposition in the hydrothermal process into separate gaseous components, which led reduced the volatile materials in hydrochar and the combustion peak value of the volatile materials. During the second stage from 360 to 460 °C, the weight loss rate of wheat straw reached a maximum at 400 °C, which was the combustion of fixed carbon in the hydrochar. Compared with wheat straw, the weight loss rate of water hyacinth reached a maximum at 450 °C. The main combustion zone moved to a higher temperature, and the maximum weight loss rate was reduced.

Because there was a volatile combustion peak and fixed carbon combustion peak on the hydrochar weight loss rate curve, it was divided into two zones with 360 °C as the boundary. According to Table 7, the activation energy of volatile combustion and fixed carbon combustion were lower than those for bituminous coal in each zone (187.6 kJ/mol and 125.9 kJ/mol) (Karcz *et al*. 1980; Cumming 1984). The activation energy of wheat straw hydrochar in the low-temperature zone was larger than that in the high-temperature zone. Due to the reduced separation of volatile materials and the greater resistance in the separation process, the activation energy increased. The activation energy of water hyacinth hydrochar in the low-temperature zone was slightly smaller than in the high-temperature zone, which indicated that fixed carbon and volatile materials burned at the same time. The activation energy of water hyacinth was appreciably higher than wheat straw, which indicated that water hyacinth was more carbonized by hydrothermal carbonization, which led to combustion difficulties and increased activation energy.

Table 7. Kinetics Properties of Wheat Straw and Water Hyacinth Hydrochar Combustion

Biomass	Temperature (°C)	n	Weight Loss (wt. %)	A (s^{-1})	E_a (kJ/mol)	R	E_m (kJ/mol)
Wheat Straw	270-360	1	20.80	2.4×10^2	44.20	0.9912	37.38
	360-420	1	18.58	9.6	29.74	0.9980	
Water Hyacinth	270-360	1	7.65	6.4×10^2	44.96	0.9910	51.26
	360-450	1	15.97	5.9×10^3	54.28	0.9993	

R: sample correlation coefficient

CONCLUSIONS

1. Under the same reaction conditions with different biomass sample sources, the physicochemical characteristics of hydrochar obtained by the hydrothermal method were quite different. Due to the differences in the three biomass components, the quality and energy yields of hydrochar of cotton stem were the highest, and those of water hyacinth were the lowest. With regard to physicochemical characteristics, the hydrochar of all biomass materials was rich in oxygen-containing functional groups. Water hyacinth hydrochar also showed good structure characteristics, as the carbon spheres were observed in SEM images.

2. With increasing temperature, the quality and energy yields of the hydrochar were reduced. At about 240 °C, the surface structure of hydrochar created more microspheres and more developed and looser pores.
3. Under different heating rates, the pyrolysis of wheat straw and water hyacinth primarily occurred at 200 to 500 °C. When the weight loss values were the same, the pyrolysis temperature at high heating rate increased, and the activity energy of hydrochar at two weight loss stages decreased. Hydrochar mainly experienced volatile materials combustion and fixed carbon combustion. The activation energy of wheat straw was about 37 kJ/mol, whereas that of water hyacinth was about 51 kJ/mol.

ACKNOWLEDGEMENTS

The authors express their sincere appreciation to the National Nature Science Foundation of China (51406063 and 51376075), the Special Fund for Agro-Scientific Research in the Public Interest (201303091), and the Postdoctoral Foundation of China (2014M552053).

REFERENCES CITED

Antonietti, M., and Titirici, M.-M. (2010). "Coal from carbohydrates: The 'chimie douce' of carbon," *CR Chim.* 13(1-2), 167-173. DOI: 10.1016/j.crci.2009.02.005

Cao, X., Ro, K. S., Libra, J. A., Kammann, C. I., Lima, I., Berge, N., Li, L., Li, Y., Chen, N., and Yang, J. (2013). "Effects of biomass types and carbonization conditions on the chemical characteristics of hydrochars," *J. Agric. Food Chem.* 61(39), 9401-9411. DOI: 10.1021/jf402345k

Coats, A., and Redfern, J. (1964). "Kinetic parameters from thermogravimetric data," *Nature* 201(4 Jan. 1964), 68-69. DOI: 10.1038/201068a0

Cumming, J. W. (1984). "Reactivity assessment of coals *via* a weighted mean activation energy," *Fuel* 63(10), 1436-1440. DOI: 10.1016/0016-2361(84)90353-3

Funke, A., and Ziegler, F. (2010). "Hydrothermal carbonization of biomass: A summary and discussion of chemical mechanisms for process engineering," *Biofuel Bioprod. Bior.* 4(2), 160-177. DOI: 10.1002/bbb.198

Gao, Y., Wang, X. H., Yang, H. P., and Chen, H. P. (2012). "Characterization of products from hydrothermal treatments of cellulose," *Energ.* 42(1), 457-465. DOI: 10.1016/j.energy.2012.03.023

Gao, Y., Wang, X., Wang, J., Li, X., Cheng, J., Yang, H., and Chen, H. (2013). "Effect of residence time on chemical and structural properties of hydrochar obtained by hydrothermal carbonization of water hyacinth," *Energy* 58(1 Sept. 2013), 376-383. DOI: 10.1016/j.energy.2013.06.023

Heilmann, S.M., Davis, H.T., Jader, L.R., Lefebvre, P.A., Sadowsky, M.J., Schendel, F.J., Keitz, M.G., and Valentas K.J. (2010). "Hydrothermal carbonization of microalgae," *Biomass Bioenerg.* 34(6), 875-882. DOI: 10.1016/j.biombioe.2010.01.032

Harun, M., Dayang Radiah, A. B., Zainal Abidin, Z., and Yunus, R. (2011). "Effect of physical pretreatment on dilute acid hydrolysis of water hyacinth (*Eichhornia* *crassipes*),” *Bioresource Technol.* 102(8), 5193-5199. DOI: 10.1016/j.biortech.2011.02.001

He, C., Giannis, A., and Wang, J. Y. (2013). “Conversion of sewage sludge to clean solid fuel using hydrothermal carbonization: Hydrochar fuel characteristics and combustion behavior,” *Appl. Energ.* 111(Nov. 2013), 257-266. DOI: 10.1016/j.apenergy.2013.04.084

Hu, B., Wang, K., Wu, L., Yu, S. H., Antonietti, M., and Titirici, M. M. (2010). “Engineering carbon materials from the hydrothermal carbonization process of biomass,” *Adv. Mater.* 22(7), 813-828. DOI: 10.1002/adma.200902812

Kang, S., Li, X., Fan, J., and Chang, J. (2012). “Characterization of hydrochars produced by hydrothermal carbonization of lignin, cellulose, D-xylose, and wood meal,” *Ind. Eng. Chem. Res.* 51(26), 9023-9031. DOI: 10.1021/ie300565d

Karcz, H., Kordylewski, W., and Rybak, W. (1980). “Evaluation of kinetic parameters of coal ignition,” *Fuel* 59(11), 799-802. DOI: 10.1016/0016-2361(80)90259-8

de Koning, H. W., Smith, K., and Last, J. (1985). “Biomass fuel combustion and health,” *B. World Health Organ.* 63(1), 11-26.

Kumar, A., and Huhnke, R. (2014). “Biomass thermochemical conversion technologies for production of fuels, power and chemicals,” in: *Compendium of Bioenergy Plants: Switchgrass*, H. Lou, L. Wu, and C. Kole (eds.), CRC Press, Boca Raton, FL, USA, pp. 295-314.

Kumar, S., Kothari, U., Kong, L., Lee, Y., and Gupta, R. B. (2011). “Hydrothermal pretreatment of switchgrass and corn stover for production of ethanol and carbon microspheres,” *Biomass Bioenerg.* 35(2), 956-968. DOI: 10.1016/j.biombioe.2010.11.023

Liu, Z., and Balasubramanian, R. (2014). “Upgrading of waste biomass by hydrothermal carbonization (HTC) and low temperature pyrolysis (LTP): A comparative evaluation,” *Appl. Energ.* 114(Feb. 2014), 857-864. DOI: 0.1016/j.apenergy.2013.06.027

Nizamuddin, S., Jayakuma, N. S., Sahu, N. Y., Ganesan, P., Bhutto, A. W., and Mubarak, N. M. (2015). “Hydrothermal carbonization of oil palm shell,” *Korean J. Chem. Eng.* 32(9), 1789-1797. DOI: 10.1007/s11814-014-0376-9

Nizamuddin, S., Mubaraka, N. M., Tiripathic, M., Jayakuma, N. S., Sahud, J. N., and Ganesan, P. (2016). “Chemical, dielectric and structural characterization of optimized hydrochar produced from hydrothermal carbonization of palm shell,” *Fuel.* 163(1), 88-97. DOI: 10.1016/j.fuel.2015.08.057

Nunes, L., Matias, J., and Catalao, J. (2013). “Economic evaluation and experimental setup of biomass energy as sustainable alternative for textile industry,” in: *Power Engineering Conference (UPEC), 2013 48th International Universities,* Sept. 2-5, 2013, Dublin, Ireland, 6 pp. DOI:10.1109/UPEC.2013.6714907

Peterson, A. A., Vogel, F., Lachance, R. P., Fröling, M., Antal, Jr. M. J., and Tester, J. W. (2008). “Thermochemical biofuel production in hydrothermal media: A review of sub-and supercritical water technologies,” *Energ. Environ. Sci.* 1(1), 32-65. DOI: 10.1039/b810100k

Poerschmann, J., Weiner, B., Wedwitschka, H., Baskyr, I., Koehler, R., and Kopinke, F-D. (2014). “Characterization of biocoals and dissolved organic matter phases obtained upon hydrothermal carbonization of brewer’s spent grain,” *Bioresource Technol.* 164(July), 162-169. DOI: 10.1016/j.biortech.2014.04.052

Roberts, J. J., Cassula, A. M., Prado, P. O., Dias, R. A., and Balestieri, J. A. P. (2015). "Assessment of dry residual biomass potential for use as alternative energy source in the party of General Pueyrredón, Argentina," *Renew. Sust. Energ. Rev.*, 41(Jan.), 568-583. DOI: 10.1016/j.rser.2014.08.066

Sheng, C., and Azevedo, J. (2005). "Estimating the higher heating value of biomass fuels from basic analysis data," *Biomass Bioenerg.* 28(5), 499-507. DOI: 10.1016/j.biombioe.2004.11.008

Turmanova, S. C., Genieva, S. D., Dimitrova, A. S., and Vlaev, L. T. (2008). "Non-isothermal degradation kinetics of filled with rise husk ash polypropene composites," *Exp. Polym. Lett.* 2(2), 133-146. DOI: 10.3144/expresspolymlett.2008.18

Xiao, L.-P., Shi, Z.-J., Xu, F. and Sun, R. C. (2012). "Hydrothermal carbonization of lignocellulosic biomass: Chemical and structural properties of the carbonized products," in: *Proceedings of the 55th International Convention of Society of Wood Science and Technology*, Beijing, China, paper SP-14.

Yang, H., Yan, R., Chen, H., Lee, D. H., and Zheng, C. (2007). "Characteristics of hemicellulose, cellulose and lignin pyrolysis," *Fuel* 86(12-13), 1781-1788. DOI: 10.1016/j.fuel.2006.12.013

Yu, Y., Lou, X., and Wu, H. (2007). "Some recent advances in hydrolysis of biomass in hot-compressed water and its comparisons with other hydrolysis methods," *Energ. Fuel* 22(1), 46-60. DOI: 10.1021/ef700292p

Zhao, P., Shen, Y., Ge, S., Chen, Z., and Yoshikawa, K. (2014). "Clean solid biofuel production from high moisture content waste biomass employing hydrothermal treatment," *Appl. Energ.* 131(15 Oct. 2014), 345-367. DOI: 10.1016/j.apenergy.2014.06.038

Article submitted: January 8, 2016; Peer review completed: February 27, 2016; Revisions received: March 8, 2016; Revisions accepted: March 15, 2016; Published: March 18, 2016.
DOI: 10.15376/biores.11.2.4113-4133